Erin A. Henslee[1]
Michael B. Sano[1]*
Andrea D. Rojas[2]*
Eva M. Schmelz[3]
Rafael V. Davalos[1,2]

[1]School of Biomedical Engineering and Sciences, Virginia Tech-Wake Forest University, Blacksburg, VA, USA
[2]Department of Materials Science and Engineering, Virginia Tech, Blacksburg, VA, USA
[3]Department of Human Nutrition, Foods and Exercise, Virginia Tech, Blacksburg, VA, USA

Received January 27, 2011
Revised May 2, 2011
Accepted May 2, 2011

Research Article

Selective concentration of human cancer cells using contactless dielectrophoresis

This work is the first to demonstrate the ability of contactless dielectrophoresis (cDEP) to isolate target cell species from a heterogeneous sample of live cells. Since all cell types have a unique molecular composition, it is expected that their dielectrophoretic (DEP) properties are also unique. cDEP is a technique developed to improve upon traditional and insulator-based DEP devices by replacing embedded metal electrodes with fluid electrode channels positioned alongside desired trapping locations. Through the placement of the fluid electrode channels and the removal of contact between the electrodes and the sample fluid, cDEP mitigates issues associated with sample/electrode contact. MCF10A, MCF7, and MDA-MB-231 human breast cells were used to represent early, intermediate, and late-staged breast cancer, respectively. Trapping frequency responses of each cell type were distinct, with the largest difference between the cells found at 20 and 30 V. MDA-MB-231 cells were successfully isolated from a population containing MCF10A and MCF7 cells at 30 V and 164 kHz. The ability to selectively concentrate cells is the key to development of biological applications using DEP. The isolation of these cells could provide a workbench for clinicians to detect transformed cells at their earliest stage, screen drug therapies prior to patient treatment, increasing the probability of success, and eliminate unsuccessful treatment options.

Keywords:
Clausius–Mossotti factor / Dielectrophoresis / Enrichment / Microfluidics / Sample isolation
DOI 10.1002/elps.201100081

1 Introduction

Dielectrophoresis (DEP) has been increasingly investigated as a method for particle separation and isolation. The potential of DEP as a biological tool for sample isolation and enrichment for drug screening, disease detection and treatment, as well as on-chip applications lies in its inherent advantages over current concentration and detection techniques. These techniques typically maintain an inverse relationship between specificity and sensitivity forcing the compromise of high-throughput and highly specific isolation. Concentration methods such as density gradient-based centrifugation or filtration [1], fluorescent and magnetic-activated cell sorting (FACS/MACS) [2, 3] and laser tweezers [4], as well as detection techniques such as PCR and immunochemistry are all examples that demonstrate this basic problem encountered by the current detection techniques. Commonly, the more sensitive techniques may require prior knowledge of cell-specific markers and antibodies to prepare target cells for analysis. Additionally, the complex sample handling required by these techniques may compromise gene expression, contaminate samples, reduce cell populations, as well as add to experimental time and cost [5].

Since DEP response, the resultant motion of a particle due to its polarization in a non-uniform electric field [6, 7], is dependent upon physical and electrical properties of a particle, it presents an advantage over the current techniques in the ability to be highly specific with minimal sample preparation. Several applications to isolate target cells based on their biophysical properties have been successfully demonstrated through the separation of leukemia, breast cancer, and other targeted cells from blood [8–10], cancer cells from $CD34^+$ hematopoietic stem cells [11],

Correspondence: Dr. Rafael V. Davalos, School of Biomedical and Engineering Sciences, Virginia Tech-Wake Forest University, 329 ICTAS Building, Stanger Street (MC 0298) Blacksburg, VA 24061 Office, USA
E-mail: davalos@vt.edu
Fax: +1-540-231-9738

Abbreviations: AC, alternating current**; cDEP,** contactless dielectrophoresis**; DEP,** dielectrophoresis**; iDEP,** insulator-based dielectrophoresis

*These authors contributed equally to this work.

Colour Online: See the article online to view Figs. 1,3,4 in colour.

neuroblastoma cells from HTB glioma cells [10], as well as cervical carcinoma cells [8], K562 human CML cells [12], and mammalian cells based on their cell-cycle phase [13, 14]. The selectivity of DEP has been further demonstrated through the distinction of cells of the same type based on their activation state [15, 16].

Insulator-based DEP (iDEP) was investigated as a means to simplify the fabrication process of more traditional DEP methods relying on patterned electrodes within the sample channel, making DEP more appealing for mass production. iDEP relies on a direct current (DC) voltage, or low-frequency alternating current (AC) voltage, applied across the sample channel, where insulating structures within the microfluidic channel create the electric field non-uniformities necessary for DEP, as opposed to the electrode geometry required in traditional DEP [17–19]. Since these insulating structures typically traverse the entire depth of the channel, a greater area of the sample channel is affected by the gradient of the inner product of the electric field, greatly improving the device throughput. In addition, the DC field creates electrokinetic flow across the length of the sample channel, alleviating the need for a pump in pressure-driven flow [18, 20–28].

Contactless dielectrophoresis (cDEP) is a promising new DEP technique [29] that exploits the intrinsic advantages of DEP, while also mitigating the challenges associated with sample/electrode contact in the traditional DEP and iDEP. Rather than metal electrodes, cDEP utilizes fluid electrodes to develop electric field non-uniformities within a separate sample channel. The fluid electrode channels, containing a high-conductive solution, are isolated from the sample channel by thin insulating membranes [29, 30]. The geometry of the fluid electrode channels as well as the sample channel, which incorporates insulating barriers, creates the electric field non-uniformities necessary for DEP. This technique eliminates cell–electrode contact, minimizing contamination of the biological sample, joule heating, bubble formation, as well as electrochemical effects [29, 30]. As with iDEP, cDEP lends itself to mass fabrication techniques such as hot embossing and injection molding. cDEP has successfully been proven able to trap particles and selectively isolate viable leukemia cells from non-viable cells [29, 30].

This study is the first to assess the ability of cDEP to distinguish viable cell types. Specifically, trapping frequencies of human breast cancer cells representing early, intermediate, and advanced stages of the disease were determined for a range of voltages. The DEP responses of MCF10A, MCF7, and MDA-MB-231 cells were investigated using a cDEP device previously shown to isolate viable from non-viable human leukemia cells [30]. This study, through theoretical modeling, numerical simulations, and experimental results, demonstrates the ability of this particular cDEP device to distinguish dielectric properties of breast cancer at various stages. Additionally, this study can be used as a platform to further cDEP development towards applications such as isolation of cells from the same lineage, detection techniques, and individualized medicine.

2 Theory

DEP is the motion of a particle due to its polarization within a non-uniform electric field and is dependent on a particle's physical and electrical properties. By exploiting these differences in various cell types, DEP can be used as a method for separation. Different cells will have varying DEP responses to the same gradient of the inner product of the electric field determined by Pohl [6, 7]

$$F_{\mathrm{DEP}} = 2\pi\varepsilon_{\mathrm{M}} r^3 \mathrm{Re}\{K(\omega)\}\nabla(E \cdot E) \tag{1}$$

where ε_{M} is the permittivity of the suspending medium, r is the radius of the particle, and E is the root mean-square electric field. $\mathrm{Re}\{K(\omega)\}$ is the real part of the Clausius–Mossotti factor given by

$$K(\omega) = \frac{\varepsilon_{\mathrm{p}}^* - \varepsilon_{\mathrm{M}}^*}{\varepsilon_{\mathrm{p}}^* + 2\varepsilon_{\mathrm{M}}^*} \tag{2}$$

where $\varepsilon_{\mathrm{p}}^*$ and $\varepsilon_{\mathrm{M}}^*$ are the complex permittivities of the particle and the medium, respectively. Complex permittivity is defined as

$$\varepsilon^* = \varepsilon + \frac{\sigma}{j\omega} \tag{3}$$

where ε and σ are the real permittivity and conductivity of the subject, $\mathrm{j} = \sqrt{-1}$ and ω is the radial frequency. From the single shell dielectric model [31] the effective permittivity and conductivity of the particle (ε_{p} and σ_{p} respectively) can be expressed as

$$\varepsilon_{\mathrm{p}} = \varepsilon_{\mathrm{m}} \frac{\gamma^3 + 2\left(\frac{\varepsilon_{\mathrm{c}} - \varepsilon_{\mathrm{m}}}{\varepsilon_{\mathrm{c}} + 2\varepsilon_{\mathrm{m}}}\right)}{\gamma^3 - \left(\frac{\varepsilon_{\mathrm{c}} - \varepsilon_{\mathrm{m}}}{\varepsilon_{\mathrm{c}} + 2\varepsilon_{\mathrm{m}}}\right)} \tag{4}$$

$$\sigma_{\mathrm{p}} = \sigma_{\mathrm{m}} \frac{\gamma^3 + 2\left(\frac{\sigma_{\mathrm{c}} - \sigma_{\mathrm{m}}}{\sigma_{\mathrm{c}} + 2\sigma_{\mathrm{m}}}\right)}{\gamma^3 - \left(\frac{\sigma_{\mathrm{c}} - \sigma_{\mathrm{m}}}{\sigma_{\mathrm{c}} + 2\sigma_{\mathrm{m}}}\right)} \tag{5}$$

where the subscripts m and c denote membrane and cytoplasm respectively and $\gamma = (r/r{-}d)$ where r is the particle radius and d is the membrane thickness. By substituting Eqs. (4) and (5) into Eq. (3), the real part of Clausius–Mossotti factor in Eq. (2) is given by

$$\begin{aligned}\mathrm{Re}[K(\varepsilon_{\mathrm{p}}^*, \varepsilon_{\mathrm{M}}^*, \omega)] = &\frac{(\sigma_{\mathrm{p}} - \sigma_{\mathrm{M}})}{(1+\omega^2\tau_{\mathrm{MW}}^2)(\sigma_{\mathrm{p}} + 2\sigma_{\mathrm{M}})} \\ &+ \frac{\omega^2\tau_{\mathrm{MW}}^2(\varepsilon_{\mathrm{p}} - \varepsilon_{\mathrm{M}})}{(1+\omega^2\tau_{\mathrm{MW}}^2)(\varepsilon_{\mathrm{p}} + 2\varepsilon_{\mathrm{M}})}\end{aligned} \tag{6}$$

where $\tau_{\mathrm{MW}} = \frac{\varepsilon_{\mathrm{p}} + 2\varepsilon_{\mathrm{M}}}{\sigma_{\mathrm{p}} + 2\sigma_{\mathrm{M}}}$ is the Maxwell–Wagner relaxation time.

It is important to note that $\mathrm{Re}\{\mathrm{K}(\omega)\}$ can take both positive and negative values based on the sign of Eq. (6). When the particle is more polarizable than the medium, the particle will move toward regions containing the highest gradient of the inner product of the electric field (positive DEP). If the medium is more polarizable than the particle, the electric field will be distorted around the particle inducing the dipole in the opposite direction pushing the particle away from regions containing the highest gradient of the

inner product of the electric field (negative DEP). The frequency at which the force changes direction is known as a crossover frequency. At this frequency, the medium and particle have the same complex permittivity and thus there is no net force on the particle. By using the relation Re{K(ω)}, unknown dielectric properties can be determined from particles' DEP responses [32–34]. Conversely, if dielectric properties of a particle are known, the crossover frequency can be calculated and exploited for separation of one particle type from a heterogeneous sample [8, 9, 11, 13, 14, 16, 35].

3 Methods

3.1 Device fabrication

A silicon master stamp was fabricated on a <100> working-grade silicon substrate (University Wafer, South Boston, MA, USA). The wafer was coated with AZ 9260 photoresist (AZ Electronic Materials, Branchburg, NJ, USA) and exposed to UV light through a chrome-plated glass mask for 45 s with an intensity of 12 W/m. To remove the exposed photoresist, a potassium-based buffered developer AZ 400K (AZ Electronic Materials) was used. The silicon master stamp was etched to 50 μm using Deep Reactive Ion Etching (Alcatel Micro Machining Systems, Annecy, France). Silicon oxide was grown on the master stamp using thermal oxidation for 4 h at 1000°C and removed with buffered oxide etch (BOE) solvent. This was repeated twice to adequately reduce surface scalloping and reduce adhesion of the polymer replicas.

Replicas of the master stamp were molded using polydimethylsiloxane (PDMS). Liquid-phase PDMS was made using a 10:1 ratio of the PDMS monomers and curing agent (Sylgrad 184, Dow Corning, USA) respectively. Once degassed, the liquid PDMS was poured onto the silicon wafer and cured for 45 min at 100°C. Upon cooling, the PDMS mold was peeled from the master stamp, fluidic connections were punched using 1.5 mm hole punchers (Harris Uni-Core, Ted Pella, Redding, CA, USA) and excess PDMS was cut off. The PDMS mold was then bonded to cleaned 3×3 cm microscope glass slides after treating with air plasma for 2 min.

3.2 Cell preparation

For these experiments, established human cell lines that represent the broad spectrum of breast cancer disease were used. As a model for non-transformed cells, MCF10A (ATCC, Manassas, VA, USA) cells were chosen. MCF10A is a spontaneously immortalized breast epithelial cell line that expresses breast-specific antigens and normal breast epithelial markers, such as cytokeratin and milk fat globule antigen, but shows only the modest gene alterations found in cultured cells. MCF10A do not form tumors in mice, thus serve as the non-transformed control. Intermediate stages were represented by the MCF7 (ATCC, Manassas, VA, USA) cells that express the estrogen receptor. Aggressive, metastatic disease was represented by MDA-MB-231 (ATCC) human breast cancer cells.

Cells were cultured in DMEM/F12 media (Invitrogen, Grand Island, NY, USA). For MDA-MB-231 and MCF7 cells, the medium was supplemented with 10% fetal bovine serum (Invitrogen, Grand Island, NY, USA) and 1% of a penicillin/streptomycin (Invitrogen) solution. In addition, the MCF7 medium was suppplemented with 0.5 nM estradiol (Sigma-Aldrich, Saint Louis, MO, USA) and 2 mL of 2.5 mg/mL insulin (Sigma-Aldrich). MCF10A medium contained 5% horse serum (Invitrogen), 1% penicillin/streptomycin solution, and 2 mL of 2.5 mg/mL insulin, 0.215 mL of 50 μg/mL epidermal growth factor (Sigma-Aldrich), 0.1 mL of 2.5 mg/mL hydrocortisone (Sigma-Aldrich), and 100 ng/mL cholera toxin (Sigma-Aldrich). All cells were cultured at 37°C in 5% CO_2 in a humidified atmosphere.

All cells were harvested by trypsinization at 80% confluence. Each cell type was resuspended in DEP buffer [30], washed twice, and resuspended again in fresh DEP buffer to achieve a solution conductivity of 100 μS/cm and a cell concentration of 10^6 cells/mL. They were then pipetted with a 300 μL pipetter to reduce cell clumping. Fifty cell radii for each cell type were measured from a calibrated image of the cells under a microscope slide. Initially, each cell type was tested individually to measure their frequency and voltage responses, then a new sample of cells for each type were stained with either calcein AM or CellTrace™ calcein red/orange (Invitrogen, Eugene, OR, USA) and mixed together to evaluate the extent of cDEP separation.

3.3 Experimental set-up

The devices were placed into a vacuum jar for at least 30 min prior to experiments. To reduce fouling in the pillar region of the device, the main channel was primed with a filtered DEP solution containing 5% BSA for 1 h. The channel was then washed with DEP buffer using pressure-driven flow. Side channels were filled with PBS and aluminium electrodes were placed in each side channel inlet (Fig. 1). Teflon tubing was inserted into the inlet and outlet of the main channel. The inlet tubing was connected to a 1 mL syringe containing the cell suspension. The syringe was fastened to a syringe pump set to 0.02 mL/h. A calibrated, inverted light microscope (Leica DMI 6000B, Leica Microsystems, Bannockburn, IL, USA) was used to monitor the cells. Once the flow rate was maintained for 5 min, an AC electric potential was applied to the electrodes.

Experiments to determine initial DEP response and at least 90% trapping were conducted at $20V_{rms}$, $25V_{rms}$, $30V_{rms}$, $35V_{rms}$, $40V_{rms}$, and $50V_{rms}$ for each cell line. These voltages were chosen due to the absence of an observed DEP force on the cells below $20V_{rms}$, while above $50V_{rms}$, no trapping distinction could be observed. For each experiment, the frequency was adjusted by intervals of 2 kHz until

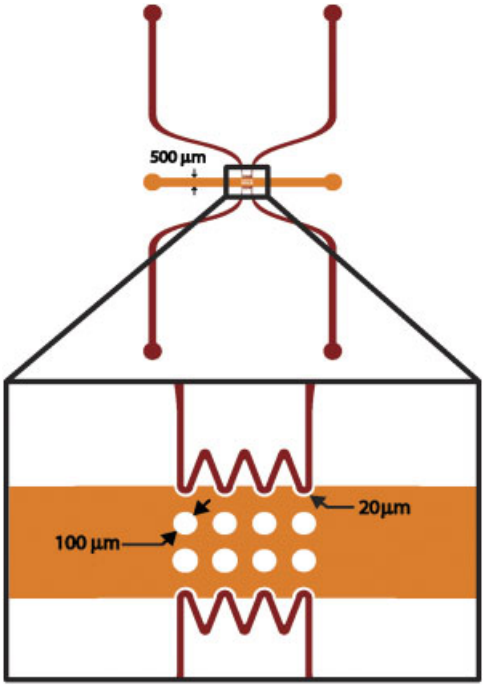

Figure 1. Schematic of experimental device. The side channels are filled with high-conductive PBS.

an initial DEP response was observed. Similarly, 90% trapping was measured by initial observation. After each initial observation at 90%, ±5 kHz were also tested. Thirty second video footage was captured for each trial and replayed in slow motion while the amount of cells flowing in and out of the trapping region were counted. Eight trials were conducted at each voltage in a random order.

3.4 Numerical modeling

The real part of the Clausius–Mossotti factor, $K(\omega)$, was theoretically calculated and graphed for each cell line using a MATLAB script (R2010a, The MathWorks, Natick, MA). The Clausius–Mossotti factor was found for frequencies between 100 Hz and 100 MHz using a logarithmic sampling rate in MATLAB with the parameters in Table 1.

The gradient of the inner product of the electric field was modeled using COMSOL Multiphysics (3.5a, COMSOL, Burlington, MA, USA). The electrical potential, ϕ, was found using the governing equation, $\nabla \cdot (\sigma^* \nabla \phi) = 0$, where σ^* is the complex conductivity $\sigma^* = \sigma + j\omega\varepsilon$ of the sub-domains in the microfluidic devices. The sub-domains were grouped into three areas: fluid electrode, sample channel, and PDMS, where the conductivities of these materials are 1.4 S/m, 1.0×10^{-2} S/m, and 8.3×10^{-13} S/m, respectively. The permittivity used for the fluid electrode and the sample channel was $80\varepsilon_0$ while the permittivity of the PDMS was $2.65\varepsilon_0$. The boundary conditions used were prescribed uniform potentials at the inlets of one fluid electrode and ground at the inlets of the other fluid electrode.

4 Results

Experimentally, the onset of cell trapping from MDA-MB-231 cells occurred at voltages as low as $20V_{rms}$ when a minimum frequency of 174.67 kHz was applied. As the applied voltage increased, the frequency necessary to induce cell trapping decreased, reaching a minimum of 125.78 kHz when $50V_{rms}$ was applied. Similarly, 90% of MDA-MB-231 cells could be trapped at $20V_{rms}$ when a minimum frequency of 267.93 kHz was applied. This decreased to a frequency of 176.02 kHz when $50V_{rms}$ was applied.

At $20V_{rms}$, the onset of cell trapping did not occur for MCF7 cells until a 209.97 kHz signal was applied. Complete trapping of these cells at this voltage was not seen until at least 302.76 kHz was applied. Similar to the MDA-MB-231 cells, the frequency necessary for the onset and 90% trapping thresholds could be reduced by increasing the applied voltage. At $50V_{rms}$, these frequencies had dropped to a minimum of 131.48 and 198.67 kHz respectively.

At all voltage levels, MCF10A required the highest average applied frequency to induce trapping and achieve 90% or greater trapping (Fig. 2). At $20V_{rms}$ this corresponded to minimum of 224.67 and 311.00 kHz, respectively. At $50V_{rms}$ a minimum of 130.39 kHz was needed to induce trapping and 208.81 kHz was required to trap at least 90% of the MCF10A cells.

The largest zone in which only MDA-MB-231 cells were influenced by DEP forces occurred at 20 and $30V_{rms}$. In this region, it was possible to isolate MDA-MB-231 cells from a heterogeneous mixture of MCF7 and MCF10A cells as shown in Fig. 2. At $20V_{rms}$ this region was approximately between 180 and 210 kHz. For $30V_{rms}$, the bandwidth was slightly smaller falling approximately between 155 and 175 kHz. Experimentally, voltages greater than $50V_{rms}$ occasionally induced cell lysing. Voltages about $65V_{rms}$ typically caused the formation of defects within the insulating barriers, which negatively altered the device performance.

Table 1. Literature values of cell dielectric properties. Cell radii and media conductivity were experimentally measured

Cell type	Average radius (µm)	Membrane capacitance (F/m^2)	Cytoplasm conductivity (S/m)	Cytoplasm permittivity (F/m)	Media conductivity (S/m)	Media permittivity (F/m)
MCF10A	9.25	0.0194 [40]	1 [41]	$50\varepsilon_0$ [41]	1.00E−02	$80\varepsilon_0$
MCF7	9.1	0.0186 [40]	1 [41]	$50\varepsilon_0$ [41]	1.00E−02	$80\varepsilon_0$
MDA-MB-231	8.93	0.0163 [40]	1 [41]	$50\varepsilon_0$ [41]	1.00E−02	$80\varepsilon_0$

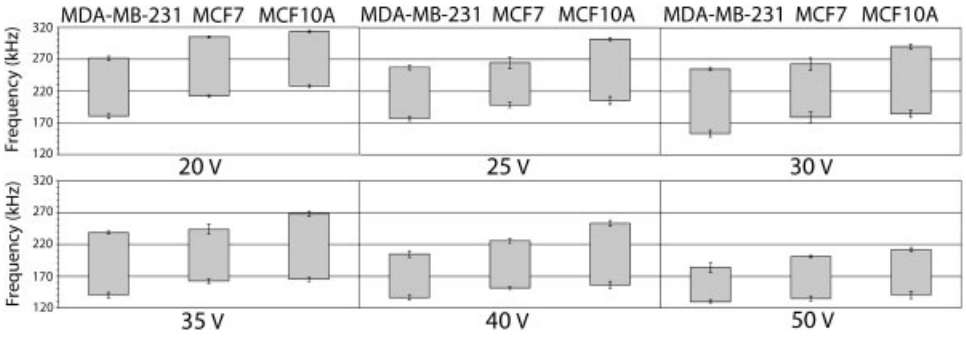

Figure 2. Frequencies between which, the onset of trapping and 90% trapping was observed for MDA-MB-231, MCF7, and MCF10A cells. At 20–30 V_{rms} MDA-MB-231 cells could be trapped while the other cell types passed through the device unaffected. The onset of trapping and 90% trapping of MCF7, MCF10A, and MDA-MB-231 cells occurred over different overlapping frequency bands.

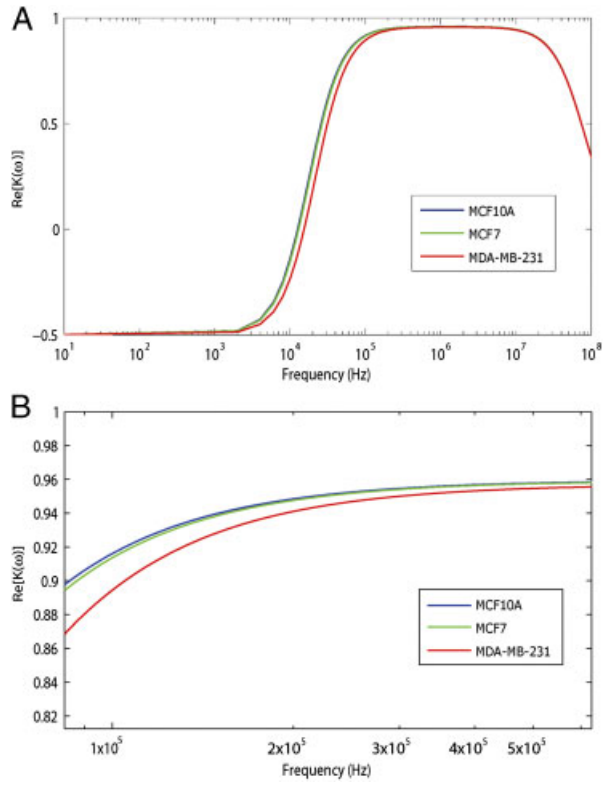

Figure 3. (A) The real part of the Clausius–Mossotti factor for MCF10A, MCF7, and MDA-MB-231 cells using estimated parameters in Table 1. (B) Zoomed in image of the curve at experimental frequencies.

The Clausius–Mossotti factor for MCF7, MCF10A, and MDA-MB-231 cells were distinct with each cell type having its own unique crossover frequency between 12.5 and 15.5 kHz. For these cells, the Clausius–Mossotti factor was within 98% of the global maxima by 200 kHz. Between 100 and 500 kHz, a unique curve of the Clausius–Mossotti factor for each cell type can be distinguished as shown in Fig. 3A and B.

Between the ranges of 100 kHz and 1 MHz, the cells experience the maximum DEP force necessary to be manipulated. In our device models, a frequency of 100 kHz was applied to demonstrate specific areas of local maxima and local minima of the DEP force (Fig. 4A). Within the sample channel, local maxima in the gradient of the inner product of the electric field were found to be in the regions closest to the left and right of the insulating pillars. The gradient of the inner product of the electric field is the greatest near the quadrants of the four inner pillars closest to $x = 0$. Local minima were found to exist at the middle of the center-to-center spacing of the pillars from left to right and top to bottom (Fig. 4A).

The DEP force acting on cells passing through the center of the device was found to have the same pattern for all of the cell types. The magnitude of the DEP force was the greatest for MCF7 cells and the lowest for MDA-MB-231 cells with MCF10 cells between the two (Fig. 4B). To validate the individual results of Fig. 2, experiments with a heterogeneous sample containing an equal number of each cell type were conducted at 30 V and at frequencies <180 kHz (frequency at which initial trapping of the MCF7 and MCF10A cells began). It was found the target cell line, MDA-MB-231, could be trapped with no trapping of the other two cell lines at 164 kHz (Fig. 4C).

5 Discussion

Current cell-sorting techniques generally suffer from a lack of sensitivity, non-specificity, and throughput. Each of these techniques relies on prior knowledge of specific cell properties for separation and has intrinsic advantages and disadvantages. Typically, more sensitive techniques may require prior knowledge of cell-specific markers and antibodies to prepare target cells for analysis. Additionally, the large amount of sample handling required by these techniques greatly increases the likeliness of cell loss and contamination, therefore increasing the error involved in the application of these techniques [5].

DEP has been shown to be a promising technique to overcome these challenges. The dielectric properties of a cell are determined by the distribution of surface charges, cell size, and morphology, as well as conductivity and permittivity of their membranes, cell walls, and internal structure. Cells are made of complex structures adjacent to one another with their own unique electrical properties. For example, the cell membrane consists of a lipid bilayer, which is a very thin insulator that contains proteins. This

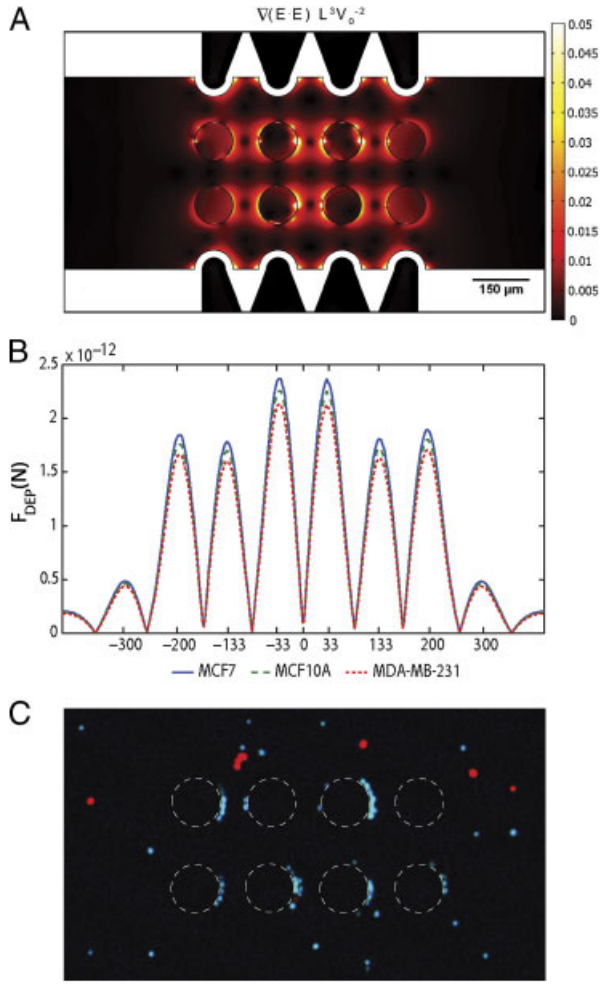

Figure 4. (A) Non-dimensionalized computational model of the gradient of the inner product of the electric field used to predict trapping regions within the cDEP device where L and V correspond to the width of the sample channel (500 μm) and the applied AC voltage (100 V_{rms}). Regions in yellow generate the highest DEP force and are the regions in which targeted cells are held. (B) DEP force on MCF7, MCF10A and MDA-MB-231 cells versus location from the center of the microfluidic channel. The DEP force within the sample channel at 100 kHz was numerically calculated to be the greatest for MCF7 cells. All cell types would experience a similar pattern of DEP forces as they traverse the device. (C) MDA-MB-231 cells (green/blue) trapping along the circumference of the insulating posts that are outlined with white dotted lines with no MCF7 or MCF10A (both red) trapping. Cells are moving from right to left under pressure-driven flow at 30 V and 164 kHz.

layer has a conductivity around 10^{-7} S/m whereas the conductivity of the inside of the cell can be as high as 1 S/m. The Clausius–Mossotti factor is a powerful parameter that relates cells' effective permittivities and conductivities to ultimately decide the magnitude and direction of DEP force. Unfortunately, the current DEP techniques suffer from their own disadvantages such as complex fabrication, cell contamination, and joule heating. For biological applications, it is crucial to overcome these hurdles. cDEP has proven to be a viable enhancement of current DEP technology through investigations of particle separation [36] as well as live/dead separation [30]. This study demonstrates the sensitivity of this current cDEP device to detect minute differences within the cell through their DEP responses.

Numerical modeling of MCF7, MCF10A, and MDA-MB-231 cells showed that the cells had unique Clausius–Mossotti curves. These curves were substantially different at frequencies near the crossover frequencies of the cells. In this region, it is likely that one cell type will experience negative DEP forces, movement away from regions containing a high gradient of the inner product of the electric field, while the others experience a positive DEP force. It should be noted however, that in this region, the magnitude of the Clausius–Mossotti factor is small in comparison to the global maximum and the resulting force experienced by the cells will be significantly lower.

Thorough examination of the cells' behavior at frequencies between 120 and 320 kHz and voltages between 20 and 50 V_{rms} showed that MDA-MB-231 cells can be isolated from a heterogeneous mixture of cells. At frequencies between 155 and 175 kHz and voltages between 20 and 30 V_{rms}, a portion of the MDA-MB-213 cells were successfully trapped while MCF7 and MCF10A cells passed by unaffected. This is the first demonstration of cDEP to isolate a specific cell type from a heterogeneous population of live cells.

Future work will focus on improving the sensitivity and removal efficiency of cDEP devices. One particular extension of this will be to investigate breast cancer cells from the same lineage, as a more clinically relevant sample mixture. Not only could this provide a basis for detection, but also the ability to isolate the most aggressive cells from a heterogeneous sample will have a profound impact on cancer therapies. The isolation of these cells could offer a workbench for clinicians to screen drug therapies prior to patient treatment, which will increase the probability of success and eliminate unsuccessful treatment options. This would enable oncologists to tailor a treatment on a patient-specific level and to ensure the most effective treatment is being utilized [37–39].

This work has been funded in part by the Institute for Critical and Applied Sciences (ICTAS) at Virginia Tech, Blacksburg, VA.

Conflict of interest: Sano and Davalos have a pending patent in Contactless Dielectrophoresis.

6 References

[1] Giddings, J., *Science* 1993, *260*, 1456–1465.

[2] Fu, A. Y., Spence, C., Scherer, A., Arnold, F. H., Quake, S. R., *Nat. Biotech.* 1999, *17*, 1109–1111.

[3] Miltenyi, S., Muller, W., Weichel, W., Radbruch, A., *Cytometry* 1990, *11*, 231–238.

[4] Ashkin, A., Dziedzic, J. M., Yamane, T., *Nature* 1987, *330*, 769–771.

[5] Adams, A. A., Okagbare, P. I., Feng, J., Hupert, M. L., Patterson, D., Gottert, J., McCarley, R. L., Nikitopoulos, D., Murphy, M. C., Soper, S. A., *J. Am. Chem. Soc.* 2008, *130*, 8633–8641.

[6] Pohl, H. A., *J. Appl. Phys.* 1951, *22*, 869–871.

[7] Pohl, H. A., *J. Appl. Phys.* 1958, *29*, 1182–1188.

[8] Cheng, J., Sheldon, E. L., Wu, L., Uribe, A., Gerrue, L. O., Carrino, J., Heller, M. J., O'Connell, J. P., *Nat. Biotech.* 1998, *16*, 541–546.

[9] Gascoyne, P. R. C., Xiao-Bo, W., Ying, H., Becker, F. F., *IEEE Trans. Indl. Appl.* 1997, *33*, 670–678.

[10] Huang, Y., Joo, S., Duhon, M., Heller, M., Wallace, B., Xu, X., *Anal. Chem.* 2002, *74*, 3362–3371.

[11] Stephens, M., Talary, M. S., Pethig, R., Burnett, A. K., Mills, K. I., *Bone Marrow Transplant.* 1996, *18*, 777–782.

[12] Altomare, L., Borgatti, M., Medoro, G., Manaresi, N., Tartagni, M., Guerrieri, R., Gambari, R., *Biotechnol. Bioeng.* 2003, *82*, 474–479.

[13] Huang, Y., Wang, X. B., Becker, F. F., Gascoyne, P. R., *Biophys. J.* 1997, *73*, 1118–1129.

[14] Kim, U., Shu, C.-W., Dane, K. Y., Daugherty, P. S., Wang, J. Y. J., Soh, H. T., *Proc. Natl. Acad. Sci. USA* 2007, *104*, 20708–20712.

[15] Toner, M., Irimia, D., *Annu. Rev. Biomed. Eng.* 2005, *7*, 77–103.

[16] Griffith, A. W., Cooper, J. M., *Anal. Chem.* 1998, *70*, 2607–2612.

[17] Cummings, E. B., Singh, A. K., *Anal. Chem.* 2003, *75*, 4724–4731.

[18] Davalos, R. V., McGraw, G. J., Wallow, T. I., Morales, A. M., Krafcik, K. L., Fintschenko, Y., Cummings, E. B., Simmons, B. A., *Anal. Bioanal. Chem.* 2008, *390*, 847–855.

[19] Baylon-Cardiel, J. L., Jesus-Perez, N. M., Chavez-Santoscoy, A. V., Lapizco-Encinas, B. H., *Lab Chip* 2010, *10*, 3235–3242.

[20] Jen, C.-P., Huang, C.-T., Shih, H.-Y., *Microsystem Technol.* 2010, *16*, 1097–1104.

[21] Ozuna-Chacón, S., Lapizco-Encinas, B. H., Rito-Palomares, M., Martínez-Chapa, S. O., Reyes-Betanzo, C., *Electrophoresis* 2008, *29*, 3115–3122.

[22] Du, F., Baune, M., Thöming, J., *J. Electrostat.* 2007, *65*, 452–458.

[23] Lapizco-Encinas, B. H., Simmons, B. A., Cummings, E. B., Fintschenko, Y., *Electrophoresis* 2004, *25*, 1695–1704.

[24] Lapizco-Encinas, B. H., Simmons, B. A., Cummings, E. B., Fintschenko, Y., *Anal. Chem.* 2004, *76*, 1571–1579.

[25] Lapizco-Encinas, B. H., Davalos, R. V., Simmons, B. A., Cummings, E. B., Fintschenko, Y., *J. Microbiol. Methods* 2005, *62*, 317–326.

[26] Lapizco-Encinas, B. H., Ozuna-Chacón, S., Rito-Palomares, M., *J. Chromatogr. A* 2008, *1206*, 45–51.

[27] Jen, C.-P., Chen, T.-W., *Biomed. Microdev.* 2009, *11*, 597–607.

[28] Masuda, S., Itagaki, T., Kosakada, M., *IEEE Trans. Indl. Appl.* 1988, *24*, 740–744.

[29] Shafiee, H., Caldwell, J. L., Sano, M. B., Davalos, R. V., *Biomed. Microdev.* 2009, *11*, 997–1006.

[30] Shafiee, H., Sano, M. B., Henslee, E. A., Caldwell, J. L., Davalos, R. V., *Lab Chip* 2010, *10*, 438–445.

[31] Jones, T. B., *Electromechanics of Particles*, Cambridge University Press,USA 1995.

[32] Arnold, W. M., Zimmermann, U., *Z Naturforsch C* 1982, *37*, 908–915.

[33] Wang, X. B., Huang, Y., Becker, F. F., Gascoyne, P. R. C., *J. Phys. D Appl. Phys.* 1994, *27*, 1571–1574.

[34] Arnold, W. M., Zimmermann, U., *J. Electrostat.* 1988, *21*, 151–191.

[35] Becker, F. F., Wang, X. B., Huang, Y., Pethig, R., Vykoukal, J., Gascoyne, P. R. C., *J. Phys. D Appl. Phys.* 1994, *27*, 2659–2662.

[36] Shafiee, H., Caldwell, J. L., Davalos, R. V., *J. Assoc. Lab. Automat.* 2010, *15*, 224–232.

[37] Tatosian, D. A., Shuler, M. L., *Biotechnol. Bioeng.* 2009, *103*, 187–198.

[38] Ntouroupi, T. G., Ashraf, S. Q., McGregor, S. B., Turney, B. W., Seppo, A., Kim, Y., Wang, X., Kilpatrick, M. W., Tsipouras, P., Tafas, T., Bodmer, W. F., *Br. J. Cancer* 2008, *99*, 789–795.

[39] Del Bene, F., Germani, M., De Nicolao, G., Magni, P., Re, C. E., Ballinari, D., Rocchetti, M., *Cancer Chemother. Pharmacol.* 2009, *63*, 827–836.

[40] Han, A., Yang, L., Frazier, A. B., *Clin. Cancer Res.* 2007, *13*, 139–143.

[41] Sancho, M., Martinez, G., Munoz, S., Sebastian, J. L., Pethig, R., *Biomicrofluidics* 2010, *4*, 022802.

